# Brillouin-light-scattering study of long-wavelength acoustic phonons in single-crystal dysprosium films

S. H. Kong,* M. V. Klein, F. Tsui, and C. P. Flynn
*Department of Physics, University of Illinois at Urbana-Champaign, 1110 West Green Street, Urbana, Illinois 61801*
(Received 5 January 1994; revised manuscript received 20 June 1994)

We have employed Brillouin scattering to investigate elastic-wave velocities as a function of temperature in Dy thin films and in bulk Dy. The single-crystal films were synthesized by molecular-beam epitaxy to ensure high crystalline and interfacial quality. Surface (Rayleigh) and guided-wave (Lamb) modes were probed by the Brillouin technique through the surface ripple-coupling mechanism. Results taken near room temperature in the paramagnetic phase agree very well with a layered-elastic model in which the materials of the samples are represented by elastic behavior using bulk single-crystal elastic data from the literature. At lower temperatures anomalies were found for samples with the thinner Dy layers: Measured wave velocities differed by up to 2% from the model predictions, and the ratio of Lamb-to-Rayleigh intensities was twice the predicted value. The anomalies coincide with the ferromagnetic transitions of the films, and they are believed to originate from coupling between the phonons and the magnetic system in the near-surface region probed by the Brillouin scattering.

## I. INTRODUCTION

An interesting coupling between magnetic and elastic properties is observed in rare-earth metals. It is made apparent in the bulk materials by the very large magnetoelastic $\sim 0.5\%$ that appear at the ferromagnetic transitions of these metals. Magnetoelastic effects of this type are of crucial importance in thin films. In recent studies of thin epitaxial crystals the epitaxial strain caused by atomic registry at the interface between the crystal and the substrate has proved to be a factor that controls the magnetic phase equilibrium[1,2] When grown stretched by 1.6% on an yttrium substrate, for example, dysprosium no longer exhibits ferromagnetism even down to the lowest temperatures. When grown compressed by 2.4% on lutecium, on the other hand, Dy has its Curie point enhanced from the bulk value of 85 to about 170 K. The elastic strain thus raises the ferromagnetic transition temperature almost up to the Néel temperature of 178 K at which the spins first order in each basal plane to form the helical antiferromagnetic phase. The Néel point itself entails little magenetostriction and is correspondingly insensitive to epitaxial strain. Bulk ferromagnetic behavior is in fact restored with increased film thickness, but only as the dimensions become macroscopic with a length scale of $0.1-1$ $\mu$m. Because all one-dimensional solutions of the elasticity equations necessarily correspond to *uniform* strains, the thickness dependences actually arise from *anelastic* behavior, and are associated with dislocation displacements or interfacial relaxation mechanisms. These interesting complications are all manifestations of the important coupling in rare-earth metals between magnetism and strain, on which the present paper is focused.

Light scattering provides a unique probe for elastic behavior on the 1-$\mu$m length scale. By Brillouin-scattering methods it is possible to determine the velocities with which Rayleigh and Love waves propagate along the surface of a metallic crystal. The character of these vibrational modes and the wavelength of the light both serve to confine the probe depth to the chosen length scale. In short they should be consistent with macroscopic measurements of the elastic constants.

Using Dy samples grown with nearly perfect surface and interfacial structures by molecular-beam epitaxy, we have performed light-scattering measurements on a high-quality Dy single crystal. The results verify that the surface wave phenomena, when observed near room temperature, do indeed agree very well with bulk elastic measurements. The comparison is far from trivial, because the sapphire substrate and buffer and seed layers required by the crystal growth enter into the determination of the mode frequencies. The room-temperature results provide an important reference point because further data taken at low temperature reveal significant discrepancies between the measurements and the predictions. The anomalous results occur at temperatures near and below that of the ferromagnetic transition, where large magnetostictive strains occur. Discrepancies of a similar magnitude do not, for example, occur at the Néel point where the paramagnetic high-temperature phase gives way to the helimagnetic phase. The most notable discrepancy is between the observed and calculated ratios of Lamb-to-Rayleigh intensities, which differed by a factor of 2 at the Curie temperature. Therefore, the focus of this paper will be on this observation.

In what follows, Sec. II provides technical information about the light-scattering measurements in Sec. II A, crystal growth and characterization in Sec. II B, and a brief mention of the theoretical technique in Sec. II C. The results of measurements on several samples are presented in Sec. III and compared with the predictions of the model. Section IV provides further discussion of these results.

0163-1829/94/50(24)/18497(8)/$06.00  

TABLE I. The thicknesses of the Dy film, Y seed layer, chemical buffer layer, and sapphire substrate for the Dy samples studied.

| Dy film | 256 Å | 450 Å | 2565 Å | 6624 Å |
|---|---|---|---|---|
| Y cap layer | none | none | 46 Å | 46 Å |
| Y seed layer | 760 Å | 600 Å | 760 Å | 760 Å |
| Buffer layer | 1010 Å, Nb | 1200 Å, Ta | 1010 Å, Nb | 1010 Å, Nb |
| Sapphire | 0.6 mm | 0.6 mm | 0.6 mm | 0.6 mm |

## II. TECHNICAL DETAILS

### A. Light-scattering experiments

The optical methods employed here were well established by earlier applications to single-layer films.[3] As a result, any complications associated with the interpretation of the light-scattering data were confined to the consequences of the multilayer film structure. The 647-nm line of a Coherent krypton ion laser provided a 100–200-mW source of single-moded power for all the scans. Dispersion of the scattered light was provided by a Sandercock Fabry Perot interferometer operating in the six-pass configuration. Further details of the experimental arrangement will be found in Ref. 4.

The dispersion of surface wave velocity with wave vector was determined over a limited range of phonon wavelengths by varying the backscattering angle, typically between 40° and 70°. This corresponds to values of the wave vector $q$ between $1.28k_L$ and $1.88k_L$, where $k_L$ is the laser photon wave vector. For homogeneous films of thickness $t$ the velocity depends on the product $tq$, and this allows the dispersion to be charted over a large continuous range, using films of several thicknesses. This simplification is lacking in the present, multiply layered films.

### B. Sample growth and characterization

The single-crystal Dy films studied in this research were grown in a Perkin Elmer 400 chamber using well-established methods of molecular-beam epitaxy. Epitaxial grade substrates of (1120) sapphire were first buffered by a 500-Å layer of single-crystal (110) Nb or Ta, on which a smooth Y(0001) seed layer then grew readily. Dy of excellent quality could then be grown to any desired thicknesses. Further details of these procedures and the optimum conditions are published elsewhere.[5] Films of thickness approximating 250, 450, 2500, and 6600 Å were grown, the latter two capped with about 50 Å of Y. Table I records the precise specifications.

A linear profilometer was used to determine the thicknesses of the films to ~5–20% and Rutherford backscattering spectroscopy provided a reduced uncertainty of ~5–10% for the 450-Å sample.

As mentioned in Sec. I, the Curie point of epitaxial Dy crystals depends on the thickness. For this reason we undertook magnetic measurements on the 450-Å film using a superconducting quantum interference device (SQUID) to obtain the magnetization as a function of temperature in a 1-kOe field (Fig. 1). The Curie point was found at 65 K, reduced from the bulk value of 85 K as expected, but somewhat greater than Kwo's results in zero field of 50 K for a 1000-Å film and 40 K for a 200-Å film.[6] The differences can be attributed mainly to the field employed in the present work.

### C. Modeling of surface wave phenomena by elastic theory

The three- and four-layer thin-film systems studied here were modeled by a generalization of the method outlined by Farnell and Adler.[7] These authors describe a method for determining the elastic eigenmodes in a single film on an semi-infinite substrate. In our case, general solutions of the elastic-wave equation are calculated for each constituent material, and the eigenmodes of the multilayer systems determined by applying the appropriate boundary conditions at each interface. In this way the dispersion curves and light-scattering spectra of this elastic model could be calculated from the known elastic constants and densities for bulk materials. The required data for single crystals of Dy, Y, Nb, Ta, and sapphire are available in the literature in sources referenced in Table II. The elastic eigenmodes were quantized and the light-scattering spectra were predicted assuming that the

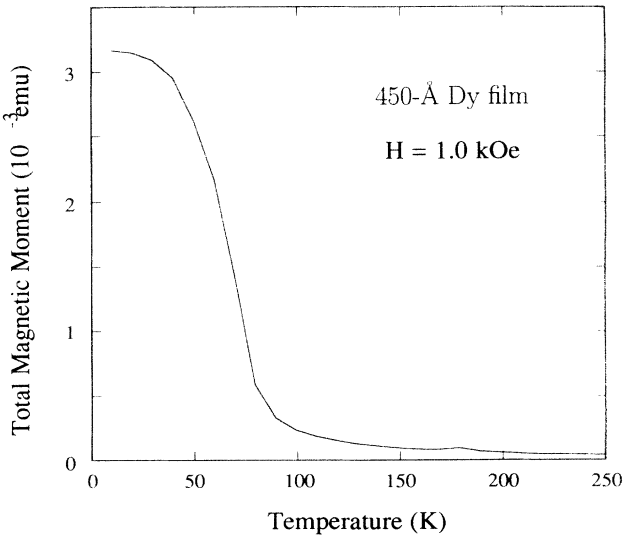


FIG. 1. The total magnetic moment of the 450-Å Dy films is plotted vs temperature. The data were taken with a SQUID magnetometer and a 1.0-kOe field was applied in the plane of the film and parallel to one of the edges of the sapphire substrate. This corresponded to a direction that is 11° from a hard axis of magnetization of Dy.

TABLE II. A listing of references for the bulk elastic constants, densities, and thermal expansion data used in the elastic model calculation for the Dy samples.

| Crystal | Elastic constants | Density | Thermal expansion |
|---|---|---|---|
| Dysprosium | Ref. 11 | Ref. 11 | Ref. 20 |
| Yttrium | Ref. 21 | Ref. 21 | Ref. 22 |
| Niobium | Ref. 23 | Ref. 23 | Ref. 23 |
| Tantalum | Ref. 24 | Ref. 25 | Ref. 26 |
| Sapphire | Ref. 27 | Ref. 28 | approximated to be 0 |

light is scattered mainly by the surface ripples induced by the acoustic modes.[8,9] The generalization of the elastic theory from a single layer to multiple layers is straightforward and will not be presented. For further detail on the calculation, refer to references 7–9 and the PAPS paper supporting this paper.[10]

## III. RESULTS

### A. Room-temperature dispersion and Brillouin spectra of the acoustic phonons in Dy films

The room-temperature study is necessary to test the predictions made by the numerical method outlined above. Although well established, the method is usually applied to a single homogeneous layer on a substrate, which is much simpler than three homogeneous layers on a substrate. Furthermore, the physical constants for the constituent materials in the layer may differ from those of the bulk materials. Good agreement of room-temperature data with model predictions for samples of different thicknesses will establish a good foundation for the temperature-dependence study and demonstrate the ability of the elastic model to predict the acoustic-phonon spectrum of a multilayer film.

Thus began a room-temperature study of a series of dysprosium films with thicknesses given in Table I. The dysprosium films grown on sapphire have two buffer layers. The dispersion of velocity no longer depends solely on the product $tq$, and the general treatment mentioned in Sec. II C is necessary. Good agreement between the calculated and experimental spectra was observed for all of the dysprosium films. However, we will only present the data for the 450-Å film since our focus will be on this sample. The data for the other samples are given in Ref. 10.

Figure 2 displays the Brillouin data for the 450-Å Dy film grown on sapphire with 600-Å Y and 1200-Å Nb buffer layers. The calculated dispersion is compared with the data points in Fig. 2(a). The data agree very well with the calculated dispersions; no adjustable parameters were introduced. Furthermore, the spectrum calculated for the ripple mechanism also compares very well with the Brillouin data in Fig. 2(b). The spectrum in Fig. 2(b) corresponds to the row of data points in Fig. 2(a) at $t_{\mathrm{Dy}}q=0.848$, where $t_{\mathrm{Dy}}=450$ Å. To incorporate instrumental resolution in the calculated spectrum, the $\delta$ functions were replaced by normalized Gaussians of width fit to the observed Rayleigh peak. The small error in the intensity of the third peak may be due either to uncertainties in the film thicknesses or to a small scattering contribution from the elasto-optic mechanism, since the relevant calculated mode is strongly longitudinal.

Note in Fig. 2(a) that there is mode mixing at several points where dispersion curves cross. We can no longer label such modes as pure Lamb or Love waves. The solid curves in Fig. 2(a) correspond to those modes that ripple the surface with at least 10% of the total displacement amplitude. These modes are Lamb, Lamb-like, Rayleigh, or mixed, but also included are some of the Love-like modes. We denote all modes in this group as Lamb-like. The remaining modes are divided into two categories. Modes that have a stronger transverse parallel component than a longitudinal component are indicated by dotted curves, and modes that have stronger longitudinal component are designated by dashed curves. These two

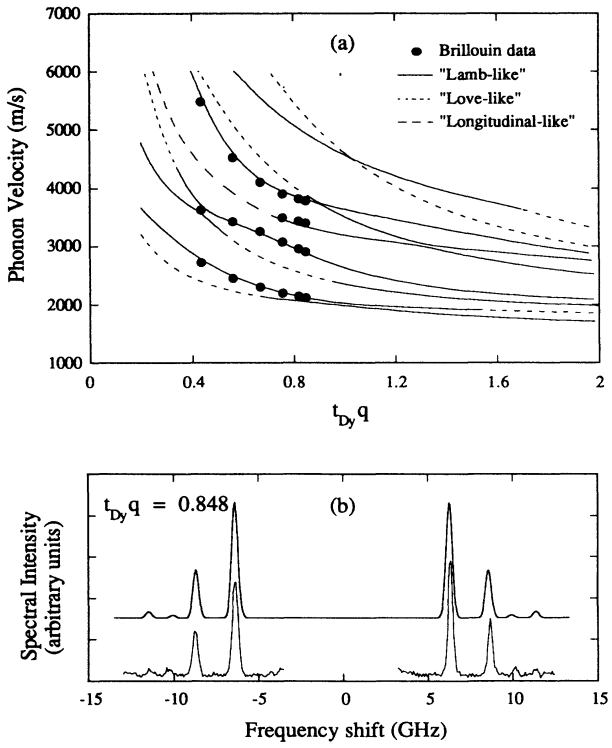


FIG. 2. Brillouin data taken from the 450-Å Dy film. (a) The observed dispersion of the phonon velocities is compared with calculated dispersion curves. (b) The Brillouin spectrum for $t_{\mathrm{Dy}}q=1.02$ (lower curve) is compared with the spectrum predicted by the ripple mechanism (upper curve). The calculated curve is offset for clarity.

groups of modes are designated Love-like and longitudinal-like, respectively. The longitudinal-like modes are actually Lamb modes with very weak transverse normal components. Modes in both of these groups weakly ripple the surface and are only observable through the ripple mechanism if the overall amplitude of the mode is sufficiently large. These groupings give rough guidance as to the observability of the modes. In what follows, a description such as Lamb-like in quotation marks refers to these groupings; without the quotation marks, Lamb-like takes its usual definition of a mixed mode that is predominantly a Lamb wave in nature.

The room-temperature study has shown that the elastic model mentioned in Sec. II C can be used to accurately predict the Brillouin spectra of multilayer metal films, in particular single-crystal dysprosium films grown on sapphire with two buffer layers. In Sec. II B, we use the same technique to model the temperature dependence of the Brillouin spectra of the 450-Å Dy film the 6624-Å Dy film, and a bulk Dy crystal.

### B. Temperature-dependence study a 6624-Å Dy film and a bulk Dy crystal

The measured temperature-dependent Rayleigh-wave velocities in the 6624-Å Dy film and in bulk Dy are compared in Fig. 3 with that Ca for bulk Dy. The calculations were made with two sets of elastic constants for Dy determined by Rosen and Klimker[11] and Palmer and Lee,[12] using an ultrasonic pulse technique.[13] The temperature dependence of the velocities for the Rayleigh waves in bulk Dy and the 6624-Å Dy film are very similar, as expected. The two experimental curves agree reasonably well with the curves calculated from the bulk elastic constants of Dy, especially since the two calculated curves do not agree exactly with each other. Most of the disagreement between the calculated curves comes from a difference in the temperature dependence of $c_{13}$ and $c_{33}$. We see from Fig. 3 that significant differences can arise between the Brillouin data and calculations using uncertain bulk elastic constants. We explore this in more detail in Sec. III C.

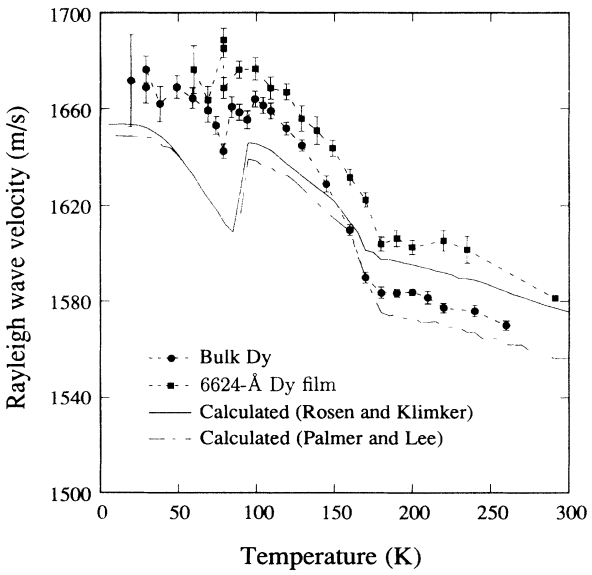


FIG. 3. Temperature dependence of the Rayleigh surface wave velocity for a Dy single-crystal slab and a 6624-Å single-crystal film determined by Brillouin scattering compared with values calculated from bulk elastic constants measured by Rosen and Klimker (Ref. 11) and Palmer and Lee (Ref. 12).

The elastic constants for an important range of temperatures are missing from the data published by Palmer and Lee. They report this as due to the very high ultrasonic attenuation near $T_c$ and to strain on the coupling media. We thus used the elastic constants determined by Rosen and Klimker for calculations modeling the Dy films. Palmer and Lee propose that the large anomalies observed in the elastic constants of bulk Dy crystals near $T_c$ are due to "rotational and domain wall processes involving reorientation of the magnetic moment vector."[12] These anomalies disappeared when they applied a 2.5-T magnetic field. As the largest magnetic field that we were able to apply was about 0.5 T, it proved impossible for us to study the regime where the anomalies in the elastic constants are suppressed.

### C. Temperature-dependence study of a 450-Å Dy film

By studying the temperature dependence of the Brillouin spectra of the 450-Å Dy film, we were able to extract the temperature dependences of the Rayleigh-wave velocity, first Lamb-like wave velocity, and the intensity of light scattering from the first Lamb-like wave relative to that from the Rayleigh wave. The spectral peaks were fit to Gaussians to model the spectral function of the interferometer. All the studies of temperature dependence in this film were performed with the angle of incidence ranging from 75° to 77° in backscattering geometry, which corresponds to $t_{\mathrm{Dy}}q=0.884$ to 0.851 for $t_{\mathrm{Dy}}=450$ Å. The backscattering angle for each scan was measured to within 0.2°, and the relative uncertainty is about 0.05° for a series of consecutive scans. $\mathbf{k}_L$ was aligned parallel to an edge of the sample. This corresponds to a phonon propagation direction 11° from the $a$ axis of the Dy film. The magnetic field was applied in the plane of the film and perpendicular to the phonon propagation direction. This corresponds to a direction that is 19° from the $a$ axis, the easy axis of magnetization. These values have uncertainties of a few degrees.

The temperature dependences of the Rayleigh-wave velocity and the first Lamb wave velocity are shown in Fig. 4. The open squares correspond to data taken without an applied magnetic field, and the filled circles denote data taken in an applied magnetic field of about 0.5 T. The field was supplied by a Nd-B-Fe permanent magnet assembly with a room-temperature magnetic field of 4.8 kOe in the gap. The magnetic field in the gap was calibrated as a function of temperature with a Hall probe. The error bars in Fig. 4 represent uncertainties in fitting the spectral peaks by Gaussians and in fitting the laser peak and the first-order ghost peaks to determine the calibration. Uncertainties in temperature have not been included. The spread of the data provides a fair indica-

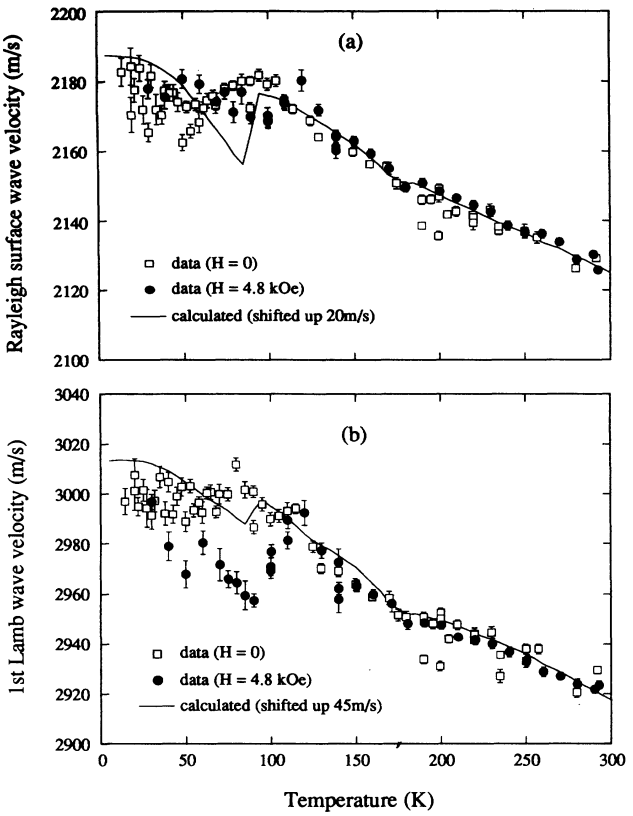


FIG. 4. Temperature dependence of (a) the Rayleigh surface wave velocity and (b) the first Lamb-like wave velocity determined from the Brillouin spectra for the 450-Å Dy film in zero field, $t_{Dy}q=0.850$ (open squares), and in a magnetic field $t_{Dy}q=0.847$ (filled circles) compared with the calculation using the temperature dependence of the zero-field elastic constants and $t_{Dy}q=0.85$.

tion of the reproducibility. At low temperatures the spectral peaks are weaker, and the reproducibility is worse. Excellent sensitivity and reproducibility are need to resolve the relatively small 1% anomaly in the phonon velocities. These experimental curves are compared with the temperature dependence calculated from the elastic model using bulk elastic constants for $H=0$ from Rosen and Klimker. Thermal expansion of the Dy film and the Ta film was taken into account using the temperature dependence of the bulk lattice constants (Table II).

Anomalies in the temperature dependence of the velocities of both phonon modes were observed near $T_c$, with and without an applied magnetic field. These anomalies occur near the Curie temperature of the film when no magnetic field is applied, and with the field on they shift up to a temperature near the Curie temperature for bulk Dy. In the absence of field, the anomalies are most difficult to resolve because the reproducibility deteriorates at low temperatures where the intensity of the spectral peaks is greatly diminished. From Refs. 11 and 12 we see that the elastic constants $c_{11}$ and $c_{12}$ for Dy exhibit large anomalous softening at the Curie temperature. This accounts for the anomalous softening present in the calculated temperature dependences, and must also contribute to the softening observed in the film. In the temperature range above the anomalies, the experimental data agree very well with the calculated curves. There are no variable parameters in the calculation. The only change that has been made is in shifting the calculated curves for the Rayleigh and Lamb-like wave velocity temperature dependences by 20 and 45 m/s respectively.

The shapes of the observed and calculated anomalies are similar. The anomalies observed in the data are less sharp, which is not surprising since the ferromagnetic transition in this film is broad (Fig. 1). It is difficult to estimate the degree of softening in the phonon velocities for $H=0$ due to the spread of the data. However, the softening observed for $H=4.8$ kOe is easier to gauge. The softening observed in the Rayleigh-wave velocity compare reasonably well with the predicted softening, but that observed in the first Lamb-like wave velocity is about three times larger than predicted. This is not unreasonable since the elastic constants probably depend on the magnetic domain structure in the film, and this is likely to differ from that of the bulk owing to the different geometry and the effects of epitaxy. Furthermore, the degree of softening also depends on the film thicknesses, which have relatively large uncertainties (5–10%). The softening of the first Lamb-like wave velocity seems particularly sensitive to the film thicknesses.

From our calculations we have observed that the Rayleigh-wave velocity is most sensitive to changes in $c_{11}$, $c_{33}$, $c_{55}$, and $c_{66}$, and the first Lamb-like wave velocity is most sensitive to changes in $c_{11}$, $c_{13}$, and $c_{33}$. Although the results do not yield quantitative elastic constants for Dy, they do show that the changes of softening may be a consequence of the differences between the temperature dependences of the elastic constants of the Dy film and bulk Dy. Since the observed softening in the Rayleigh-wave velocity is close to or slightly smaller than the calculated softening, it is unlikely that an enhanced anomaly in the temperature dependence of $c_{11}$ by itself is the cause of the discrepancy in the first Lamb-like wave velocity. However, the Rayleigh-wave velocity is insensitive to $c_{13}$. A 40% increase in $c_{13}$ at the Curie temperature can account for the observed softening in the first Lamb-like wave velocity, but it is not clear whether such an increase in $c_{13}$ is physically reasonable. A 20% decrease in $c_{33}$ would suffice, but it would also deepen the calculated anomaly in the Rayleigh-wave velocity by approximately 10 m/s. This analysis shows that moderate changes in the elastic constants of the Dy film can possibly account for the discrepancy in the depths of the anomalies.

In contrast, the intensity of light scattering from the first Lamb-like wave relative to that from the Rayleigh wave exhibits a very large anomaly in its temperature dependence. This is very difficult to explain with the elastic model, as shown in Fig. 5. This spectral intensity ratio is the ratio of the integrated intensity of the first Lamb-like peak to that of the Rayleigh-wave peak. At room temperature the calculated and observed spectral intensity ratios agree fairly well; the small discrepancy is most likely due to the uncertainties of 5–10% in the film

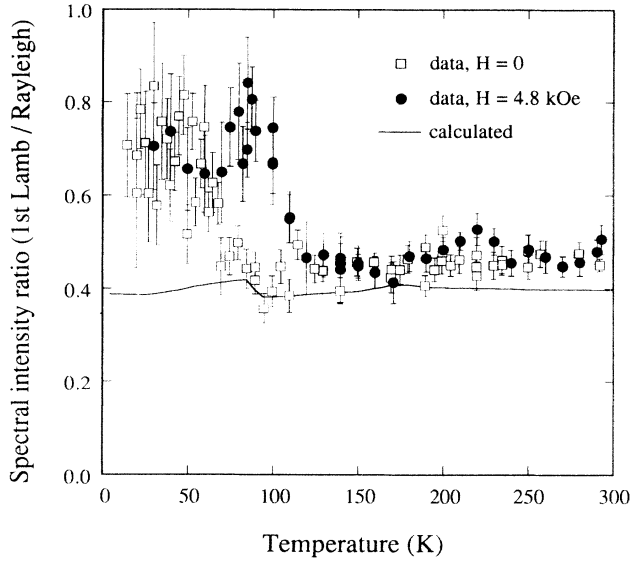


FIG. 5. For the 450-Å Dy film, the ratio of the integrated intensity of the first Lamb-like peak to that of the Rayleigh peak plotted as a function of temperature, without an applied magnetic field (open squares) and with a field applied in the plane of the film and perpendicular to the phonon propagation direction (filled circles). The data are compared with the ratios calculated from the temperature dependence of the zero-field bulk elastic constants and assuming only the ripple mechanism for light scattering.

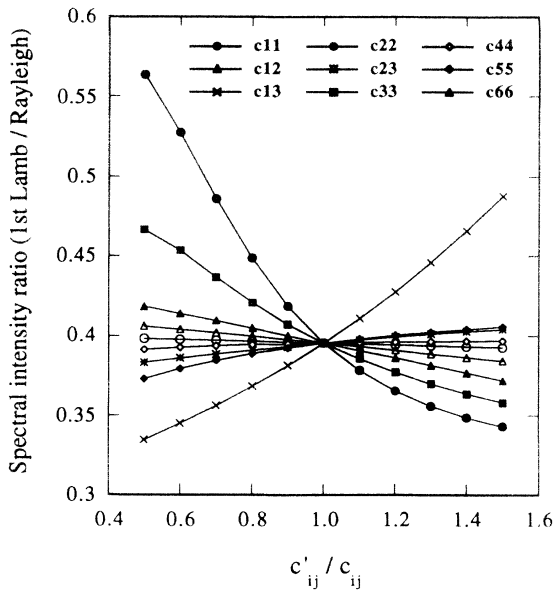


FIG. 6. Calculated ratio of the spectral intensities of the first Lamb-like wave peak and the Rayleigh wave peak for the 450-Å Dy film when each elastic constant is changed from $c_{ij}$ to $c'_{ij}$. We assume orthorhombic symmetry for the perturbed film which gives nine independent elastic constants. $c_{ij}$ are the unperturbed elastic constants at room temperature, and $c'_{ij}$ are the perturbed elastic constants.

layer thicknesses. A large discrepancy is evident in the anomalous region. The calculation predicts a peak in the spectral intensity ratio at the Curie temperature. However, the observed peak has a magnitude about seven times greater, and the ratio fails to return to its original value below the anomalous region as predicted by the calculation. It is possible that two mechanisms are acting together to give the overall enhancement.

From the calculated dependence of the spectral intensity ratio on the elastic constants of the Dy film in Fig. 6, it appears that a change of the Dy $c_{11}$ by 50% could account for approximately half of the discrepancy. Such a change is not likely since a much larger anomaly in the temperature dependence of the Rayleigh-wave velocities would then be observed. Other elastic constants of Dy could possibly change to cancel the effect of $c_{11}$ on the Rayleigh-wave velocities while not altering the spectral intensity ratio significantly, but the large coordinated changes that would be required do not appear reasonable. Note that variations of two parameters do not necessarily cause additive changes of the velocities or the spectral intensity ratio. Therefore, a thorough search through the parameter space of the elastic constants would be necessary, but hardly practical.

## IV. DISCUSSION

It is apparent that the current model cannot account for the large anomaly observed in the ratio of the Lamb-to-Rayleigh intensity for the 450-Å Dy film studied. The intensity of light scattering from an acoustic phonon is related to the amount of transverse vertical polarization in the corresponding elastic eigenmode. Thus in the following subsections we consider other factors that may perturb the relevant eigenmodes.

### A. Clamping effects

We initially considered the effect produced if the yttrium layer were to clamp the dysprosium film. In our calculations, we use the temperature dependence of the bulk elastic constants. Since the dysprosium film is epitaxially grown on yttrium, the orthorhombic distortion that accompanies magnetization may be partially or completely suppressed. A good characterization of the strains developed in the dysprosium and yttrium layers of these films is not currently available. We estimated the importance of clamping by assuming the extreme case in which the dysprosium layer is completely clamped to the yttrium layer. The strain along the $c$ axis was calculated by minimizing the magnetoelastic energy using the method outlined in Ref. 14. Using calculated third-order elastic constants from the literature for Dy,[15] we determined that the fractional difference between the elastic constants of bulk Dy and those of the clamped Dy films is $\sim 10^{-3}$ for $c_{12}$, $c_{13}$, $c_{33}$, and $c_{44}$ and $\sim 10^{-4}$ for $c_{11}$. These effects are too small to cause the observed discrepancy in the temperature dependence of the spectral intensity ratio.

In the actual system, the Dy layer probably undergoes a partial clamping with a weaker orthorhombic distortion that also strains the Y layer. This was observed for Dy/Lu superlattices.[16] Instead of modeling the strain induced in the Y layer by minimizing the total elastic and

magnetoelastic energy of the dysprosium film, including the buffer layers, we considered the extreme case where the Y layer follows the orthorhombic distortion of bulk Dy. Using the calculated third-order elastic constants for Y from the literature,[17] we find that fractional differences $\sim 10^{-3}$ for $c_{33}$ and $\sim 10^{-2}$ for $c_{11}$ and $c_{13}$ are expected between the elastic constants of bulk Y and those of the strained Y layer. Therefore, the effects of the strains induced in the Y layer are also unlikely to resolve the discrepancy.

### B. Inhomogeneity and metastability in ferromagnetic state

The effects of clamping on the ferromagnetic phase transition have not yet been considered and may be important in determining the full impact of clamping on the elastic constants of Dy. Metastable states induced by epitaxy might exist in the film near the Curie temperature. Such states are evident in Dy/Y superlattices, as can be concluded from neutron data showing that the ferromagnetic state is absent in the superlattices but is present after the application and removal of a sufficiently strong magnetic field.[18]

Metastability and inhomogeneity warrant further discussion. The ferromagnetic transition is first order and is influenced by strain. It follows that, at constant strain, there should be a mixed phase region of the phase diagram characterized by two differing values of the magnetization. The domains, which are expected to be small, will be separated by domain walls. These will be sources of dissipation and hence dispersion for elastic waves. When in addition we allow for relaxation of epitaxial strain, the system will become even more inhomogeneous.

### C. Other considerations

Further possible explanations for the large anomaly in the spectral intensity ratio are (1) the elastic properties of the regions near the interfaces should be modeled separately; (2) the first Lamb-like wave peak is enhanced or the Rayleigh-wave peak is attenuated by a magnetic excitation; or (3) the first Lamb-like wave and the Rayleigh wave become mixed as the Dy layer becomes ferromagnetic. We can only give qualitative discussions of these conjectures.

There are large lattice mismatches at the sapphire-tantalum and tantalum-yttrium interfaces, and the latter interface, at least, is not perfectly abrupt. With the addition of strain and stress induced by the Dy layer in the ferromagnetic phase, it may indeed be necessary to model the interface region separately in accordance with hypothesis (1). This explanation ignores the thinness of the interface region, for even larger changes of the elastic properties would be required to account for the large anomaly. The only interface model that could give a large change in the spectral intensity is one that assumes that the coupling between two layers through the interface is not rigid but accommodates slippage. Modeling this would require altering the interfacial boundary conditions or introducing a very soft, thin interface layer. The extreme case would correspond to complete detachment of the film with accompanying irreversible effects. We have not observed any such irreversibility in the data.

Under the second hypothesis, either a portion of the scattered light would be from a magnetic excitation, or one or both phonon modes would be altered by interaction with a magnetic excitation. We have studied the depolarized spectrum just below the Curie temperature and do not observe any peaks. This eliminates the first alternative hypothesis but may not eliminate the second, since the magnetic excitation could be too weak to observe. The acoustic magnon for Dy in the ferromagnetic phase has a very high energy of $\sim 22$ cm$^{-1}$ when the Dy magnetization is saturated.[19] However, near the transition point, the magnon energy is much lower and may coincide with the phonon energies at some temperature just below the Curie temperature. This could possibly account for the sharp peak near $T_c$, but not for the observation that the spectral intensity ratio does not return fully to its original value.

When the dispersion curves of a Lamb wave and a Love wave in the 450-Å Dy film are near a crossing, it is found from the elasticity calculations that the modes generally mix and cause the spectral intensity ratio of the peaks to fall closer to unity. The third hypothesis suggests that the Rayleigh wave and the first Lamb-like wave may mix. Since the two modes are separated by a relatively large frequency difference, this is only possible if they somehow couple through the magnetic system. In this sense, hypotheses (2) and (3) would be related. Since both phonon modes would be coupled through the magnetic system, this hypothesis requires a sufficiently strong coupling through a magnetic mode with a short enough lifetime that its frequency width encompasses both phonon modes. Near $T_c$ the magnons have short lifetimes, and again this could possibly account for an anomalous peak in the spectral intensity near $T_c$.

No firm choices can be made among these hypotheses. Better characterization of the physical structure of all three layers at low temperatures is needed. Explanations (2) and (3) require theoretical calculations to predict the response of an elastic continuum coupled to a magnetic continuum.

## V. CONCLUSIONS

We have successfully modeled the acoustic phonons in single-crystal Dy films grown on two buffer layers with a sapphire substrate for temperatures above the films' Curie temperature. We have noted excellent agreement at room temperature between the calculated and experimental phonon velocity dispersion curves for several films of varying thicknesses. We have also observed good agreement in the temperature dependence of the Brillouin spectra in a 450-Å Dy film for temperatures above the Curie temperature. However, below and at the Curie temperature of this film, a very large anomaly was observed in the temperature dependence of the scattered light intensity from the first Lamb-like wave relative to that from the Rayleigh wave that could not be accounted for by the elastic model. The scattered light intensities from these acoustic-phonon modes depend on the ampli-

tudes of the surface ripples induced by these modes. Thus the temperature dependences of the acoustic-phonon amplitudes at the surface of the film could not be modeled successfully below the Curie temperature.

The anomalous behavior of the acoustic phonons near the Curie temperature in the 450-Å Dy film is a clear indication that the dynamics of the elastic system are strongly perturbed by the ferromagnetic order in the Dy layer at and below the Curie temperature. This behavior cannot be easily modeled by solely changing the elastic constants of the Dy and Y layers to account for the influence of the magnetic order. We have suggested several possible mechanisms for the interaction between the elastic and magnetic system that may account for this anomalous behavior: We need to consider (1) the details of the static magnetic structure of the Dy film such as small domains in a metastable magnetic state which may cause acoustic phonon dissipation, and (2) the influence of the dynamics of the magnetic system through possible phonon and magnon interactions.

Similar experiments have been performed on a 500-Å Dy film grown on a Lu buffer layer instead of an Y buffer layer. Preliminary results show a similar anomalous behavior in the temperature dependence of the Brillouin spectra.

## ACKNOWLEDGMENTS

Thanks are due to Professor M. B. Salamon for helpful discussions, and to Young Lee for performing the Rutherford backscattering experiments. The Laue x-ray scattering and Rutherford backscattering was carried out in the Center for Microanalysis of Materials, Frederick Seitz Materials Research Laboratory, University of Illinois, which was supported by the U.S. Department of Energy under the Contract No. DE-AC 02-76ER01198. This work was supported by NSR DMR 85-21616 and NSF DMR 88-20888.

*Present address: Los Alamos National Laboratory, MS H825, Los Alamos, NM 87545.

[1]R. S. Beach, A. Matheny, M. B. Salamon, C. P. Flynn, J. A. Borchers, R. W. Erwin, and J. J. Rhyne, J. Appl. Phys. **73**, 6901 (1993).

[2]C. P. Flynn and F. Tsui, *Magnetism and Structure in Systems of Reduced Dimensions,* edited by R. F. C. Farrow, B. Dieny, M. Donath, A. Fert, and B. D. Hermsmeier (Plenum, New York, 1993); R. S. Beach, J. A. Borchers, A. Matheny, R. W. Erwin, M. B. Salamon, B. Everitt, K. Pettit, J. J. Rhyne, and C. P. Flynn, Phys. Rev. Lett. **70**, 3502 (1993).

[3]J. R. Sandercok, in *Light Scattering in Solids III,* edited by M. Cardona and G. Guntherodt (Springer-Verlag, Berlin, 1982).

[4]S. H. Kong, M. V. Klein, F. Tsui, and C. P. Flynn, Phys. Rev. B **45**, 12 297 (1992).

[5]J. Kwo, E. M. Gyorgy, D. B. McWhan, M. Hong, F. J. Di Salvo, C. Vettier, and J. E. Bower, Phys. Rev. Lett. **55**, 1402 (1985).

[6]J. Kwo, in *Thin Film Growth Techniques for Low Dimensional Structures,* edited by R. F. C. Furrow, S. S. P. Parkin, P. J. Dodson, J. H. Neave, and A. S. Arrott (Plenum, New York, 1987).

[7]G. W. Farnell and E. I. Adler, in *Physical Acoustics IX,* edited by W. P. Mason and R. N. Thurston (Academic, New York, 1970), p. 35.

[8]V. Bortolani, A. M. Marvin, F. Nizzoli, and G. Santoro, J. Phys. C **16**, 1757 (1983).

[9]R. Loudon and J. R. Sandercock, Phys. C **13**, 2609 (1980).

[10]S. H. Kong, M. V. Klein, F. Tsui, and C. P. Flynn, see AIP document no. PAPS PRBMDO-50-18 497-14 for 14 pages of supplementary material supporting this paper. Order by PAPS number and journal reference from the American Institute of Physics, Auxiliary Publication Service, 500 Sunnyside Boulevard, Woodbury, New York 11797-2999. The price is $1.50 for each microfiche (60 pages) or $5.00 for photocopies of up to 30 pages, and $0.15 for each additional page over 30 pages. Airmail additional. Make checks payable to the American Institute of Physics.

[11]M. Rosen and H. Klimker, Phys. Rev. B **1**, 9 (1970).

[12]S. B. Palmer and E. W. Lee, Proc. R. Soc. London Ser. A **327**, 519 (1972).

[13]H. B. Huntington, Phys. Rev. **72**, 321 (1947).

[14]B. Coqblin, *The Electronic Structure of Rare Earth Metals and Alloys: the Magnetic Heavy Rare Earths* (Academic, London, 1977), pp. 414–419.

[15]R. Ramji Rao and C. S. Menon, J. Phys. Chem. Solids **34**, 1879 (1973).

[16]R. S. Beach, J. A. Borchers, R. W. Erwin, C. P. Flynn, A. Matheny, J. J. Rhyne, and M. B. Salamon, J. Magn. Magn. Mater. **104-107**, 1915 (1992).

[17]R. Ramji Rao and A. Rajput, Can. J. Phys. **57**, 120 (1979).

[18]R. W. Erwin, J. J. Rhyne, M. B. Salamon, J. A. Borchers, S. Sinha, R. Du, J. E. Cunningham, and C. P. Flynn, Phys. Rev. B **35**, 6808 (1987).

[19]R. T. Demers, S. Kong, M. V. Klein, R. Du, and C. P. Flynn, Phys. Rev. B **38**, 523 (1988).

[20]F. J. Darnell and E. P. Moore, J. Appl. Phys. **34**, 1337 (1963).

[21]S. J. Savage, S. B. Palmer, D. Fort, R. G. Jordan, and D. W. Jones, J. Phys. F **10**, 347 (1980).

[22]R. W. Meyerhoff and J. F. Smith, J. Appl. Phys. **33**, 219 (1962).

[23]K. A. Jones, S. C. Moss, and R. M. Rose, Acta Metall. H **17**, 365 (1969).

[24]C. E. Anderson and F. R. Brotzen, J. Appl. Phys. **53**, 292 (1982).

[25]F. H. Featherston and J. R. Neighbours, Phys. Rev. **130**, 1324 (1963).

[26]F. C. Nix and D. MacNair, Phys. Rev. **61**, 74 (1942).

[27]W. E. Tefft, J. Res. Natl. Bur. Stand. Ser. A **70**, 277 (1966).

[28]W. Biltz, A. Lemke, and K. Meisel, Z. Anorg. Chem. **186**, 377 (1930).